ARTICLE OPEN

Check for updates

Adolescent methamphetamine exposure drives neuroinflammation and aberrant neurogenesis linked to anxiety and cognitive impairments in adult mice

Akane Ito[1,6], Noriyoshi Usui[1,2,3,4,5,6]✉, Miyuki Doi[1,5] and Shoichi Shimada[1,3,4,5]

The adolescent brain, characterized by its high plasticity, is particularly vulnerable to substance abuse, leading to long-term impacts on brain function and behavior. Methamphetamine (METH), a potent psychostimulant, is associated with severe neurological and psychiatric consequences. While most studies focus on METH exposure in adulthood, little is known about the effects of adolescent METH exposure. In this study, we explored the long-term effects of adolescent METH exposure on brain function and behavior in adulthood using a mouse model. Mice were administered METH for 8 days during adolescence, and their behavior was analyzed in adulthood. METH-exposed mice (METH mice) displayed anxiety-like behaviors, cognitive decline, and increased microglial numbers in the medial prefrontal cortex (mPFC) and dorsal hippocampus (dHIP). Additionally, METH exposure during adolescence induced neuroinflammation in adulthood. Adolescent METH exposure also enhances defensive reactivity to neuroinflammation and oxidative stress by activating the NFE2L2-mediated redox system and promotes neurogenesis in adulthood. These findings suggest that the detrimental effects of adolescent METH exposure extend into adulthood, emphasizing the delayed-onset impact of early exposure to psychostimulants.

Translational Psychiatry (2025)15:364; https://doi.org/10.1038/s41398-025-03613-y

INTRODUCTION

The adolescent brain is still developing, and using substances like drugs and alcohol during this crucial stage can increase the risks of harmful impacts on brain function [1–3]. The adolescent brain, characterized by its high plasticity, is more susceptible to cytoarchitectural changes compared to the adult brain. Consequently, this increases the vulnerability to substance abuse, mood swings, and cognitive impairments in adulthood [2–5]. As an example, imbalanced development of dopaminergic (DAergic) and GABAergic systems specifically affects motivation and decision-making processes [3, 6].

Being exposed to psychostimulant substances and alcohol can cause significant neurological effects, increasing the risk of developing psychiatric disorders such as addiction and substance use disorder (SUD) [7]. Data from the 2021 National Survey on Drug Use and Health (NSDUH) indicates that more than 16.8 million individuals aged 12 and above in the US, which is about 6.0% of the population, have used methamphetamine (METH) at least once in their lifetime. Recent trends show a rise in SUD among younger people, particularly men and youth, compared to women and adults, although rates decrease with age for both genders [8].

METH remains one of the most common psychostimulant substances worldwide [9]. METH, derived from amphetamine (AMPH) with a methyl group substitution, is more easily absorbed by the body than AMPH, making it more potent in pharmacological effects. The strong potency of METH makes users more prone to tolerance, overdose, addiction, dependence on psychiatric medications, and adverse health consequences.

The primary pharmacological impact of METH within the central nervous system (CNS) is the substantial alteration of dopamine (DA) dynamics in the brain. METH induces strong stimulating and euphoric effects by increasing the release of DA from storage vesicles while also blocking the dopamine transporter (DAT), which reuptakes DA [10, 11]. These neurotoxic properties of METH induce oxidative stress and neuroinflammation, eventually neuronal death and alterations in synaptic morphology [7].

Prolonged METH abuse causes a spectrum of adverse outcomes, including addiction, delusions, hypersexuality, hyperthermia, cardiac arrhythmias, heart failure, kidney failure, brain damage, severe anxiety, insomnia, depression, mood disorder, attention deficit disorder, violent behavior, schizophrenia, and cognitive decline [9, 12–17]. Anxiety emerges as a predominant symptom during METH withdrawal, particularly in the acute withdrawal phase, with its incidence correlating with the duration of METH exposure [18].

Nevertheless, while previous studies have predominantly explored the impacts of METH exposure on adult brain functions

[1]Department of Neuroscience and Cell Biology, Graduate School of Medicine, The University of Osaka, Suita, Japan. [2]Omics Center, Center of Medical Innovation and Translational Research, Graduate School of Medicine, The University of Osaka, Suita, Japan. [3]United Graduate School of Child Development, The University of Osaka, Suita, Japan. [4]Global Center for Medical Engineering and Informatics, The University of Osaka, Suita, Japan. [5]Addiction Research Unit, Osaka Psychiatric Research Center, Osaka Psychiatric Medical Center, Osaka, Japan. [6]These authors contributed equally: Akane Ito, Noriyoshi Usui. ✉email: usui@anat1.med.osaka-u.ac.jp

Received: 17 December 2024 Revised: 30 July 2025 Accepted: 1 September 2025
Published online: 06 October 2025

and behaviors, limited attention has been directed towards investigating the impacts of METH exposure during adolescence. The study focusing on adolescence has been reported that the effects of psychostimulants such as cocaine, methylphenidate, and AMPH differ between adolescent and adult mice, with adolescent mice having higher reward sensitivity to METH compared to adult mice [19]. Given that the adolescent brain is in a crucial developmental phase, comprehending the impact of stimulant substances use such as METH during this period on subsequent brain function and behavior holds significant importance.

In this study, we investigated the long-term effects of adolescent METH exposure on brain function and behavior in adulthood using a mouse model. Mice were administered METH for 8 consecutive days and their behavior was analyzed in adulthood. We found that METH-exposed mice (METH mice) exhibited anxiety-like behaviors and cognitive decline, along with increased microglial numbers in the medial prefrontal cortex (mPFC) and dorsal hippocampus (dHIP) These changes were ameliorated by treatment with minocycline (MINO), a microglial activation inhibitor. Additionally, METH exposure during adolescence induced neuroinflammation, oxidative stress response, and neurogenesis in adulthood. Our findings suggest that the adverse effects of adolescent METH exposure in brain function and behavior persist into adulthood.

MATERIALS AND METHODS

Mice

All procedures followed the ARRIVE guidelines and relevant official regulations, approved by the Animal Research Committee of The University of Osaka (#27-010). Total 91 male C57BL/6J mice (Japan SLC Inc., Shizuoka, Japan) were used in this study. Mice were housed in cages (#W140 × D320 × H140 mm, KN-60105-T, Natsume Seisakusho Co., Ltd., Tokyo, Japan) in The University of Osaka's barrier facilities under a 12 h light–dark cycle with free access to food and water. Behavioral tests were conducted between 10:00 and 17:00 h by experimenters blinded to the genotypes. The minimum number of animals for biological replicates was based on previous experiments to enable the detection of a significant difference between groups at $P < 0.05$.

METH administration

METH administration was performed as previously described [20]. Mice received a daily intraperitoneal injection of 2 mg/kg METH (#871151; Sumitomo Pharma, Osaka, Japan) dissolved in saline (#3311401A2026; Otsuka Pharmaceutical Co., Ltd., Tokyo, Japan) from P35–P42. Control (CTR) mice were given saline on the same schedule. Mouse behaviors were analyzed at 8 weeks old.

MINO administration

Mice received a daily intraperitoneal injection of 40 mg/kg MINO (#M9511; Merck, Darmstadt, Germany) dissolved in saline from P35–P42. CTR mice were also given saline on the same schedule.

Open field test

Open field test was performed as previously described [21]. Mice were placed in one of the corners of a novel chamber (W700 × D700 × H400 mm, #OF-36(M)SQ, Muromachi Kikai Co., Ltd., Tokyo, Japan) and were allowed to explore for 10 min. Locomotor activity was measured and tracked using ANY-maze behavior tracking software 7.33 (Stoelting Co., Wood Dale, IL, USA).

Marble-burying test

Marble-burying test was performed as previously described [22]. Mice were placed in the corner of a novel home cage (#KN-60105-T, Natsume Seisakusho Co., Ltd.) evenly placed eighteen marbles and allowed to explore for 20 min. The number of marbles buried was recorded. A marble was defined as buried when less than two-third of the marble was visible.

Three-chamber social behaviors test

Three-chamber social behaviors test was performed as previously described [22]. The social interaction test included three 5 min trials in a 3-chamber apparatus (W600 × D400 × H220 mm, SC-03M, Muromachi Kikai Co., Ltd.). In the first trial, mice explored the empty chambers with wire cages at each end. In the second trial, one end chamber contained a novel stranger mouse in a wire cage, while the other end chamber held an empty cage. The third trial assessed social novelty, with one end chamber containing a familiar mouse and the other a different novel stranger mouse. Interaction with the targets near the wire cages was tracked using ANY-maze (Stoelting Co.).

Novel object recognition test

Novel object recognition test was performed as previously described [22]. Mice were habituated to a chamber (#OF-36(M)SQ, Muromachi Kikai Co., Ltd.) before the test. Identical objects were placed in opposite corners of a chamber, and mice explored for 10 min. The next day, 24 h later, one object was replaced with a new shape, and mice explored again for 10 min. Object interactions were tracked using ANY-maze (Stoelting Co.). The difference score was the time spent on the novel object minus the familiar object. The discrimination ratio was the time on the novel object divided by the total exploration time.

Nest building test

Nest building test was performed as previously described [23]. Mice were provided with nest material (Happi-mats, Marshall BioResources, Ibaraki, Japan) the evening before, and the degree of nest formation was quantified the following morning using a 6-point scale.

Tail suspension test

Mice were suspended by a clip 5 mm from the tip of their tails. A 5-min test was conducted and videotaped, with immobility time manually recorded.

Forced swim test

Mice were placed in a 14 cm diameter cylinder filled with water (24–25 °C) to a depth of 16 cm. A 6-min test was conducted, with immobility recorded during the last 10 min. Immobility was defined as the absence of movement, except for minimal movements required to keep the head above water.

Immunohistochemistry

Immunohistochemistry was performed as previously described [24]. Mouse brains were fixed with 4% PFA in PBS overnight at 4 °C, cryoprotected in 30% sucrose in PBS, then embedded in Tissue-Tek O.C.T. Compound (#4583; Sakura Finetek Japan Co.,Ltd., Osaka, Japan) for cryosectioning. Cryosections (20 μm thick) were placed in PBS. Sections were incubated with the following primary antibodies overnight at 4 °C: rabbit polyclonal anti-Iba1 (1:2000; #019-19741; Fujifilm Wako Chemicals, Osaka, Japan), rat polyclonal anti-SOX2 (1:1000; #14-9811-82, Thermo Fisher Scientific, Waltham, MA, USA), rat monoclonal anti-TBR2 (EOMES) (1:500; #14-4875-82, Thermo Fisher Scientific), rat monoclonal anti-DCX (CD140a) (1:200; #14-1401-82, Thermo Fisher Scientific), and mouse monoclonal anti-Cleaved caspase-3 (1:500; #9664, Cell Signaling Technology, Danvers, MA, USA). The sections were then washed and incubated with species-specific secondary antibodies conjugated to Alexa Fluor 488 and/or Alexa Fluor 594 (1:2000; Thermo Fisher Scientific) for 1 h at room temperature. DAPI (#11034-56; Nacalai Tesque, Kyoto, Japan) was used to stain the nucleus. Cover glasses were mounted with Fluoromount/Plus (#K048, Diagnostic BioSystems, Pleasanton, CA). Images were collected using an all-in-one fluorescence microscope (BZ-X700; KEYENCE Corporation, Osaka, Japan). Cell number and area were quantified manually using ImageJ or using KEYENCE analysis software (KEYENCE Corporation).

Quantitative real-time PCR (qPCR)

qPCR was performed as described previously [25]. Total RNA was extracted from the mouse HIP at P42 and P56 or lung, liver, and kidney at P62 using the miRNeasy Mini Kit (#217004; Qiagen, Hilden, Germany) according to the manufacturer's instructions. Single-stranded cDNA was prepared using DNaseI, Amplification grade (#18068015; Thermo Fisher Scientific) and SuperScript III First-Strand Synthesis SuperMix (#18080400; Thermo Fisher Scientific) and amplified by PCR according to the manufacturer's instructions. qRT-PCR was performed using PowerUp SYBR Green Master Mix (#A25742; Thermo Fisher Scientific) and a QuantStudio 7 Flex Real-Time PCR System (Thermo Fisher Scientific). Cycling conditions were 50 °C for 2 min and 95 °C for 2 min, followed by 40 cycles at 95 °C for 1 s and

60 °C for 30 s. Each biological sample had four technical replicates for qPCR. *18S* rRNA was used as a reference for normalization. Data were analyzed by the ΔΔCq method using QuantStudio Software v1.3 (Thermo Fisher Scientific). The following primers were used: *18S rRNA*, F-5′-GAGGGAGCCTGAGAAACGG-3′, R-5′-GTCGGGAGTGGGTAATTTGC-3′; *mTnf*, F-5′-CCACCACGCTCTTCTGTCTA-3′, R-5′-AGGGTCTGGGCCATAGAACT-3′; *mIl6*, F-5′-CCGGAGAGGAGACTTCACAG-3′, R-5′-TTCTGCAAGTGCATCATCGT-3′; *mIl1b*, F-5′-TACAGGCTCCGAGATGAACA-3′, R-5′-AGGCCACAGGTATTTTGTCG-3′; *mNfe2l2*, F-5′-GCTTTTGGCAGAGACATTCC-3′, R-5′-CCAAACTTGCTCCATGTCCT-3′; *mHmox1*, F-5′-GCCACCAAGGAGGTACACAT-3′, R-5′-CTTCCAGGGCCGTGTAGATA-3 *mKeap1*, F-5′-ATGGCCACATCTACGCAGTC-3′, R-5′-CCAATCCTCCGTGTCAACAT-3′; *mNqo1*, F-5′-GAAGCTGCAGACCTGGTGAT-3′, R-5′-GTTGTCGTACATGGCAGCAT-3′.

d-ROMs (reactive oxygen metabolites) and BAP (biological antioxidative potential) tests

Mouse blood samples were collected at P42 and P56. After being kept at room temperature for 30 min, the samples were centrifuged at 1500 g for 10 min. The supernatants were collected as serum and stored at −80 °C until use. The d-ROMs and BAP were measured using REDOXLIBRA (WISMERLL, Tokyo, Japan) and d-ROMs Test kit (#DI-003b; WISMERLL) or BAP Test kit (#DI-002d; WISMERLL) according to the manufacturer's instructions, respectively.

Statistical analysis

Data are presented as means of biological independent experiments with ± standard error of the mean (SEM). Statistical analyses (unpaired *t*-test, Mann-Whitney test, or one-way ANOVA with a Tukey's multiple comparison test) were performed using Prism 9 and 10 (GraphPad Software, Boston, MA, USA). A significance level of $P < 0.05$ was considered.

RESULTS

Adolescent METH exposure caused anxiety-like behavior

To investigate the impacts of adolescent METH exposure in adulthood, we repeatedly administrated METH (2 mg/kg) to adolescent mice for 8 days at postnatal days (P) 35–P42, then analyzed the behaviors in adult at P56 (Fig. 1a). Previous studies have reported that adult METH exposure increases anxiety-like behaviors in adult mice [26, 27]. Therefore, we first examined the anxiety-like behaviors using the open field test. We found that significantly decreased the center time during the test in adolescent methamphetamine-exposed (METH) mice (Fig. 1b–h). There was no difference in the total distance traveled during the test (Fig. 1i). Thus, METH mice did not display ectopic movement (hyperactivity) in adulthood.

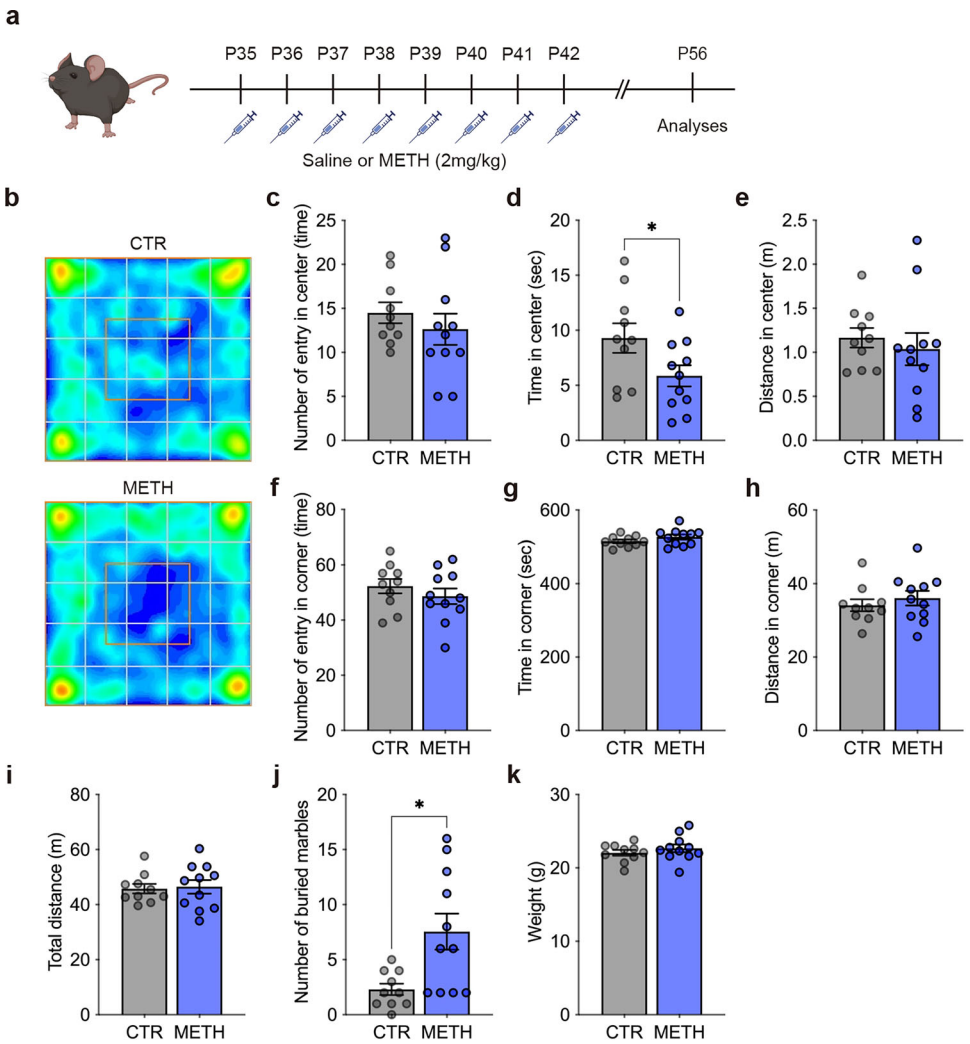

Fig. 1 Adolescent methamphetamine-exposed (METH) mice exhibited anxiety-like behavior in adulthood. a Experimental time course of METH administrations during adolescence. **b** Representative heatmaps of mouse exploratory behavior in the open field test. **c–i** Quantifications of center entry (**c**), center time (**d**), center distance (**e**), corner entry (**f**), corner time (**g**), corner distance (**h**), and total distance travelled (**i**) in the open field test. **j** Quantification of the number of buried marbles in the marble-burying test. **k** Quantification of body weight in mice. Adolescent METH mice exhibited anxiety-like behavior compared to control (CTR) mice. Data are represented as means (±SEM). Asterisk indicates *$P < 0.05$, unpaired *t*-test and Mann-Whitney test, n = 10–11/condition.

We also conducted the marble-burying test to see if anxiety-like behaviors could be evaluated using another behavioral test. We found that increased the number of buried marbles during the test in METH mice (Fig. 1j). On the other hand, there was no difference in stereotyped behaviors (data not shown), thus marble-burying test was used as an indicator for anxiety-like behaviors. There was no difference in the mouse weight (Fig. 1k). These results indicate that adolescent METH exposure increased anxiety-like behaviors in adulthood.

Adolescent METH exposure impaired short-term memory and cognitive behavior

To examine whether the adolescence METH exposure impaired other brain function, we performed social behaviors using the 3-chamber social behaviors test. We also confirmed that METH mice did not display hyperactivity during test (Supplementary Fig. 1). During the social interaction session, both CTR and METH mice exhibited normal social interaction (Fig. 2a–d, e–g). In contrast, CTR mice also exhibited normal social novelty (Fig. 2a, h–j). However, impaired social novelty was found in METH mice (Fig. 2a, k–m). These results indicate that adolescent METH exposure does not impair social interaction behaviors, but in social novelty.

Accordingly, we next evaluated cognitive function in METH mice. In the novel object recognition test, METH mice displayed decreased novel object recognition compared to CTR mice (Fig. 2n–p). During the training session, we confirmed that METH mice did not exhibit hyperactivity or any preference for specific objects (Supplementary Fig. 1 and 2). Furthermore, we performed nest building test related to cognitive and social impairments, emotion, and DAergic dysfunction [28], and found that decreased nest building in METH mice (Fig. 2q, r). These results indicate that adolescent METH exposure impairs short-term memory and cognitive function in adulthood.

Adolescent METH exposure did not cause depressive-like behavior

We also examine whether adolescent METH exposure leads to cause depression-like behavior through increased anxiety and DAergic dysfunction. We conduced tail suspension test and forced swim tests, and found that decreased immobile time in tail suspension test in METH mice, but not in forced swim test (Supplementary Fig. 3). In our experimental design, adolescent METH exposure did not cause depressive-like behaviors in adulthood.

Increased microglia induced by neuroinflammation

To investigate whether adolescent METH exposure affects the adult neural circuits, we analyzed mPFC and dHIP controlling emotion and cognition. Previous studies have reported that the METH exposure in the rodents induced oxidative stress and inflammation in the brain, eventually leading to cell death [11, 29]. We found increased IBA1-posivitve (+) microglia in the cingulate cortex area 1 (Cg1) and prelimbic cortex (PrL) regions of mPFC in METH mice compared to CTR mice (Fig. 3a–c), but not in the infralimbic cortex (IL) (Fig. 3a, d). In addition, these microglia exhibited hyper-ramified, bushy, and amoeboid morphology [30, 31], indicating the reactive microglia (Supplementary Fig. 4).

We also found increased IBA1+ microglia in the CA1, CA2, CA3 and dentate granule (DG) regions of dHIP in METH mice compared to CTR mice (Fig. 3e–i). In contrast, there was no difference in the numbers of IBA1+ microglia in the DG of METH mice at P42 (Supplementary Fig. 5). These results indicate that adolescent METH exposure increased microglia in the mPFC and dHIP only in adulthood.

We also found that no differences in the number of IBA1+ microglia in other brain regions including dorsomedial striatum, nucleus accumbens, and basolateral amygdala (Supplementary Fig. 6). Although the mechanism behind the significant increase in IBA1+ microglia in the PFC and HIP remains unclear, suggesting that there may be brain regions that are more susceptible to being affected during adolescence.

Next, we further examined whether the increase in microglia caused by adolescent METH exposure was due to neuroinflammation. We found that increased expression of proinflammatory cytokine genes such as *Tnf* and *Il6* in the HIP of METH mice at P42, but not in *Il1b* (Fig. 4a–c). In addition, continuous *Tnf* expressions was also observed in the HIP of METH mice at P56, but not in *Il6* and *Il1b* (Fig. 4d–f). These results suggest that neuroinflammation is induced immediately after adolescent METH exposure and it still continues 2 weeks after.

Adolescent METH exposure increased defensive reactivity to oxidative stress

We examined whether adolescent METH exposure induced oxidative stress. We quantified redox states in the serum of METH mice using markers d-ROMs (reactive oxygen metabolites) and BAP (biological antioxidative potential) for oxidation level and antioxidant level, respectively. We found that no change in the serum d-ROMs, BAP, and BAP/d-ROMs ratio (antioxidant capacity) in adolescent METH mice at P42 (Fig. 4g–i). Interestingly, we found decreased d-ROMs and an increased BAP/d-ROMs ratio in the serum of adult METH mice at P56, while BAP levels remained unchanged (Fig. 4j–l).

To investigate the mechanism underlying changes in redox status in adulthood, we analyzed the expression of genes associated with the oxidative stress response. We found increased mRNA expressions of *Keap1* and *Hmox1* in the HIP of METH mice at P42, but not in *Nfe2l2* and *Nqo1* (Fig. 4m–p). We also found increased mRNA expressions of not only *Keap1* and *Hmox1, but also Nfe2l2* and *Nqo1* in the HIP of METH mice at P56 (Fig. 4q–t). Moreover, we observed increased mRNA expressions such as *Nfe2l2* and *Nqo1* in the lung, liver, and kidney of adult METH mice (Supplementary Fig. 7), indicating that oxidative stress induced by adolescent METH exposure represents a systemic alteration.

These results also suggest that adolescent METH exposure alters the body's redox state, enhancing its defense against subsequent oxidative stress.

Enhancement of HIP neurogenesis in adult METH mice

We further investigated whether neuroinflammation and increased microglia affects adult neurogenesis in adulthood. We found no difference in SOX2+ neural stem cells, but a decrease in TBR2+ progenitors in the DG of METH mice at P42 (Fig. 5a–c). A trend toward an increase in DCX+ progenitors was observed in METH mice at P42 (Fig. 5a, d). Furthermore, we observed an increase in SOX2+ neural progenitors and a trend toward a decrease in TBR2+ progenitors in the DG of METH mice at P56 (Fig. 5a, e, f). There was no difference in DCX+ progenitors at P56 (Fig. 5a, g).

On the other hand, no increase in cell death in the DG of METH mice was observed at either P42 or P56 (Supplementary Fig. 8), indicating that high-dose METH-induced dramatic cell death was not observed in our experimental system.

Together, these results indicate that neurogenesis was enhanced after a period of methamphetamine use, not immediately afterward.

Inhibition of microglia activation ameliorated METH-induced phenotypes

Lastly, to investigate whether inhibiting microglial activation induced by adolescent METH exposure would ameliorate the phenotype, we administered MINO (40 mg/kg) on the same schedule as METH and investigated the phenotype of METH mice in adulthood (Fig. 6a). We found that MINO treatment attenuated anxiety-like behaviors in METH mice in the marble-burying test (Fig. 6b). We also observed MINO treatment attenuated cognitive

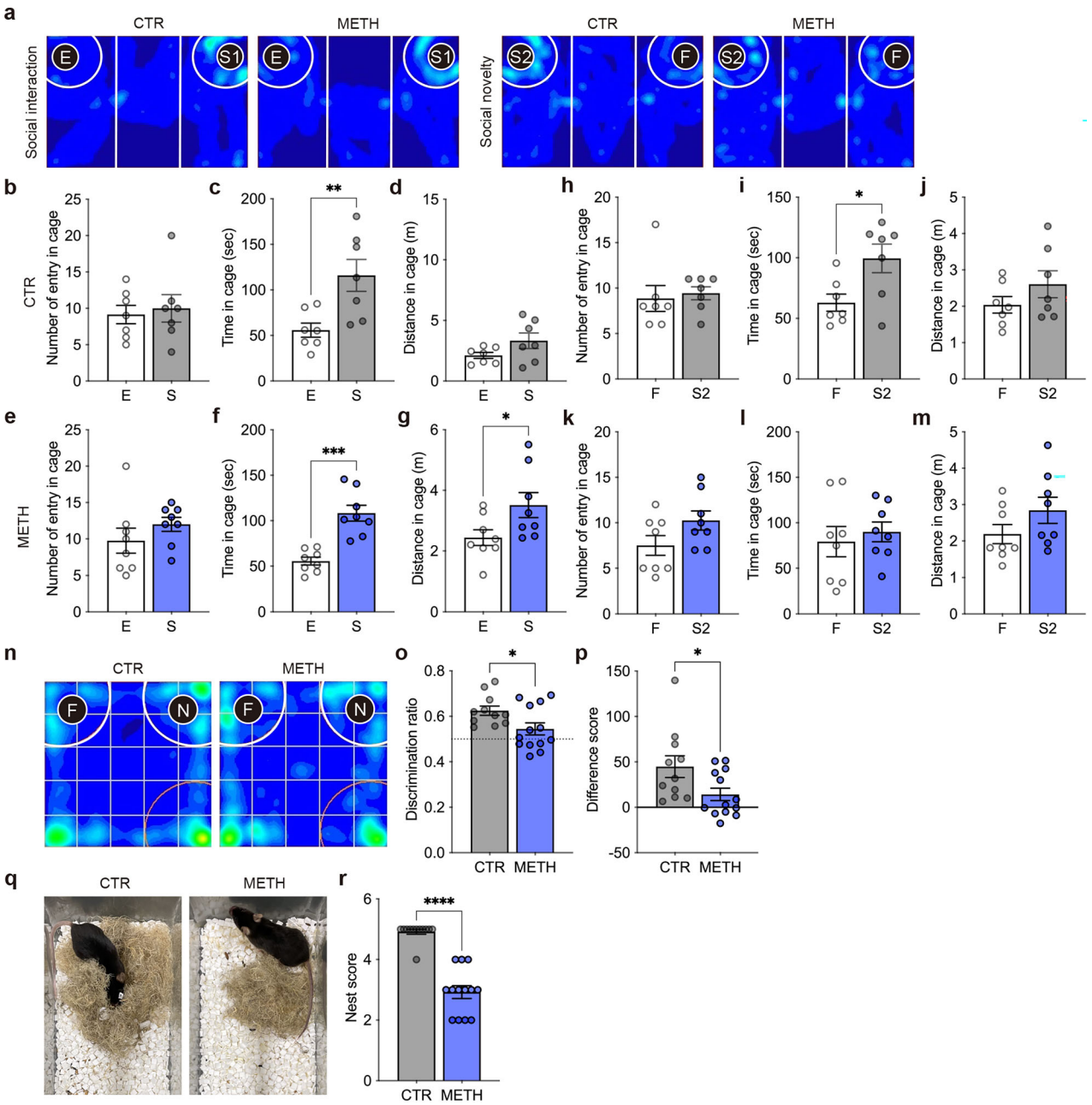

Fig. 2 Adolescent METH mice impaired cognitive function in adulthood. a Representative heatmaps of mouse social interaction and social novelty in the 3-chamber social behaviors test. *E: empty, S1: stranger mouse 1, S2: stranger mouse 2, F: familiar mouse*. **b**–**g** Quantifications of entry (**b, e**), time (**c, f**), distance (**d, g**) around the targeting cage. **h**–**m** Quantifications of entry (**h, k**), time (**i, l**), distance (**j, m**) around the targeting cage. METH mice exhibited normal social interaction, but impaired social novelty. **n** Representative heatmaps of exploratory behavior in the novel object recognition test. *F: familiar object, N: novel object*. **o, p** Quantifications of discrimination ratio (**o**) and difference score (**p**). METH mice impaired novel object recognition. **q** Representative images of mouse nests in the nest building test. **r** Quantification of nest score. M. Data are represented as means (±SEM). Asterisks indicate ****P < 0.0001, ***P < 0.001, **P < 0.01, *P < 0.05, unpaired *t*-test and Mann-Whitney test, n = 7–8/condition for 3-chamber social behaviors test, n = 11–13/condition for novel object recognition test, n = 12–13/condition for nest building test.

impairments in METH mice in the nest building test (Fig. 6c). There were no differences in the mouse weight (Fig. 6d).

Accordingly, we examined whether microglia activation was effectively inhibited by MINO treatment. As we expected, the METH-induced increase in IBA1+ microglial numbers was ameliorated in mice treated with MINO (Fig. 6e, f). We further investigated whether aberrant adult neurogenesis induced by adolescent METH exposure could also be ameliorated. Notably, MINO treatment attenuated the altered neurogenesis observed in METH mice (Fig. 6e, g).

These results indicate that inhibition of microglia activation by MINO ameliorates the behavioral and histological abnormalities related to anxiety and cognitive impairment induced by adolescent METH exposure.

DISCUSSION

In this study, we demonstrate that adolescent METH exposure leads to anxiety and cognitive impairments in mouse adulthood.

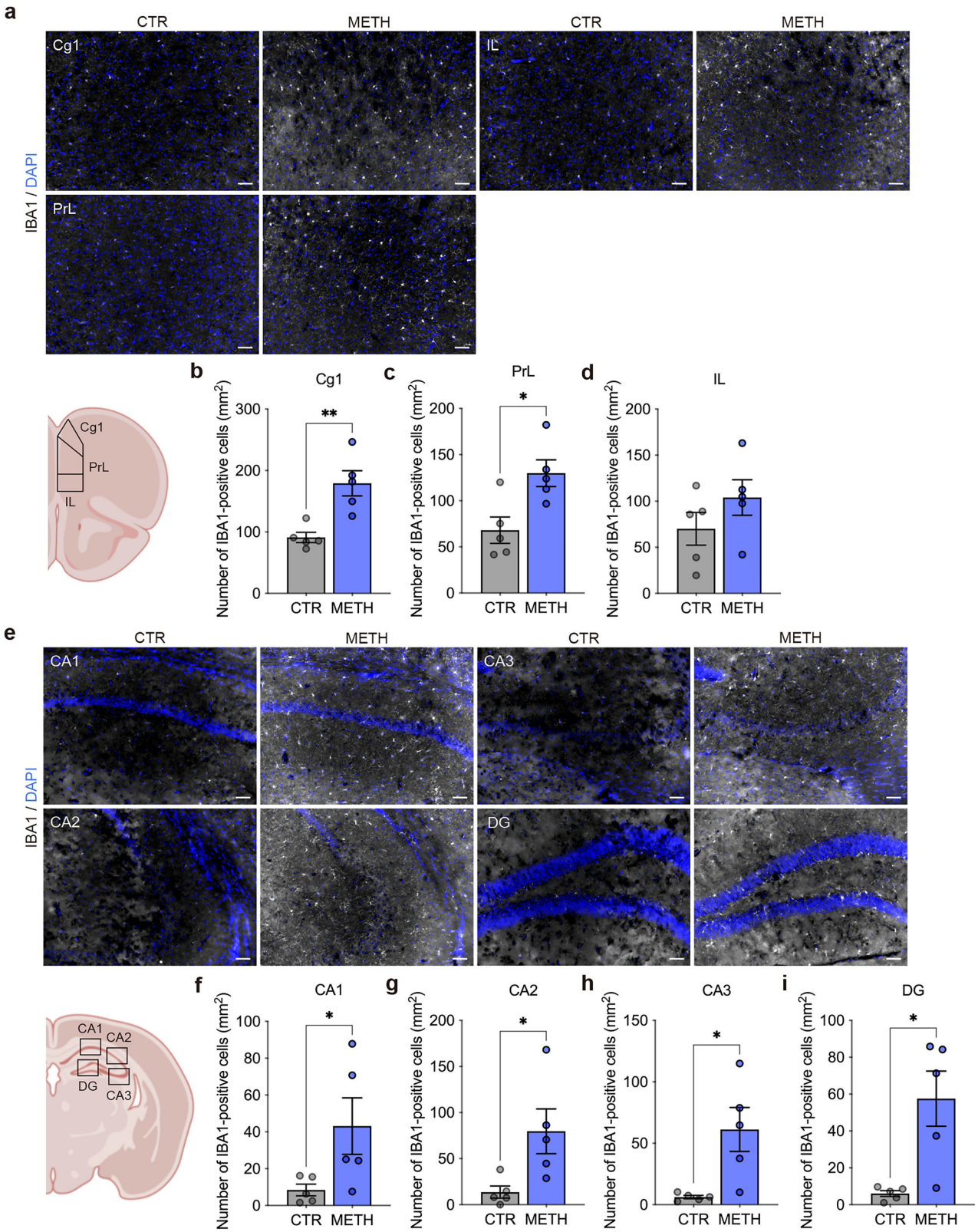

Fig. 3 Adolescent METH exposure increased the numbers of microglia in adult METH mice. a Representative fluorescence images of the mouse mPFC at P56. **b**–**d** Quantifications of IBA1-positive (+) microglia in the cingulate cortex area 1 (Cg1) (**b**), prelimbic cortex (PrL) (**c**), and infralimbic cortex (IL) (**d**). The numbers of microglia were increased in the mPFC of METH mice. **e** Representative fluorescence images of the mouse dHIP at P56. **f**–**i** Quantifications of IBA1+ microglia in the CA1 (**f**), CA2 (**g**), CA3 (**h**), and dentate granule (DG) (**i**). The numbers of microglia were also increased in the dHIP of METH mice. Data are represented as means (±SEM). Asterisks indicate **P < 0.01, *P < 0.05, unpaired *t*-test and Mann-Whitney test, n = 5/condition. Scale bars: 50 μm.

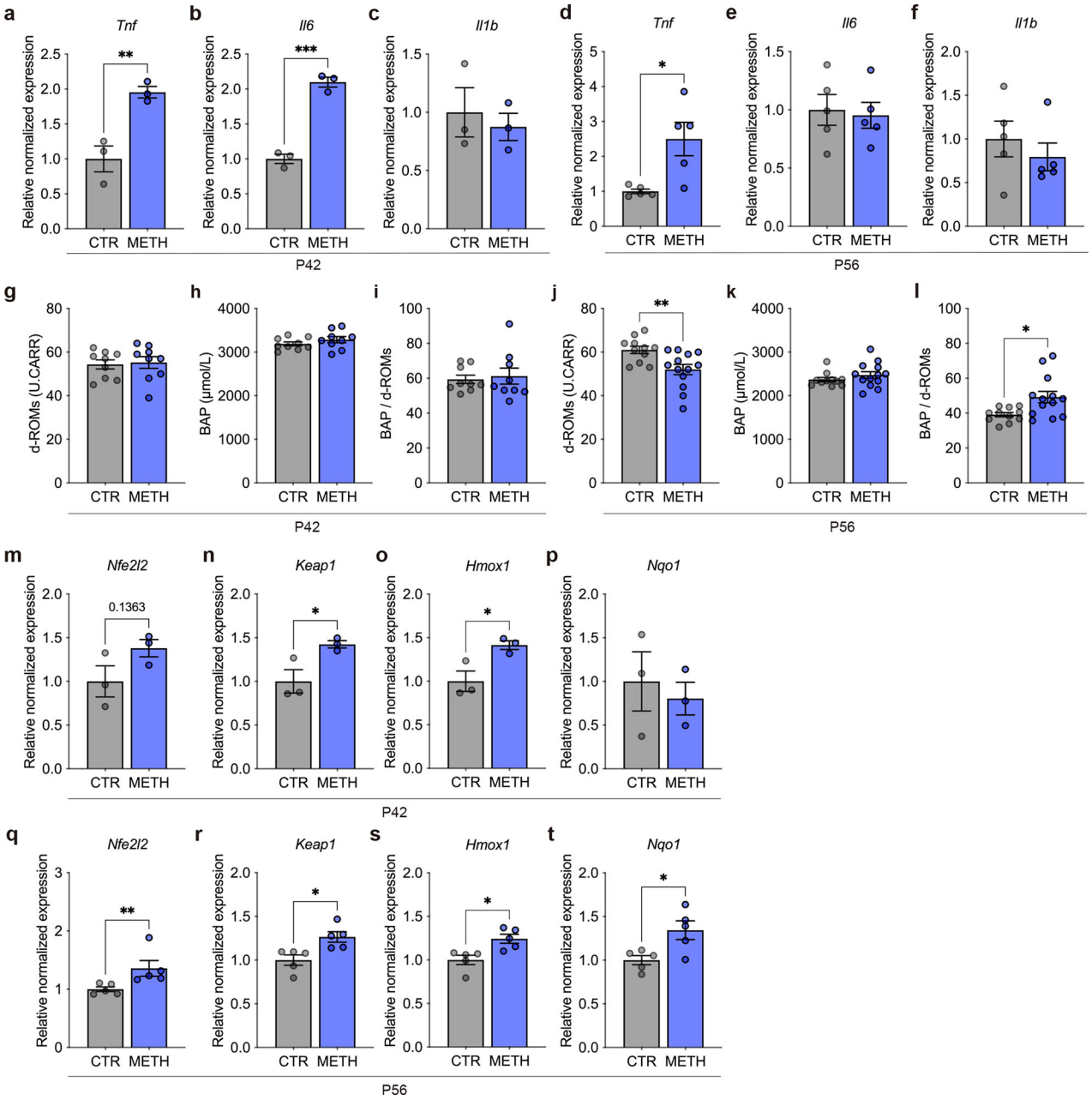

Fig. 4 Adolescent METH exposure induced inflammation and oxidative stress response. a–f Quantifications of mRNA expressions of *Tnf* (**a, d**), *Il6* (**b, e**), and *Il1b* (**c, f**) in the mouse HIP at P42 (**a–c**) and P56 (**d–f**). The expressions of inflammation-related genes were increased in the HIP of METH mice at P42 and P56 due to adolescent METH exposure. **g–i** Quantifications of d-ROMs (**g**), BAP (**h**), and BAP/d-ROMs (**i**) at P42. **j–l** Quantifications of d-ROMs (**j**), BAP (**k**), and BAP/d-ROMs (**l**) at P56. Antioxidant capacity was elevated in METH mice at two weeks after METH exposure. **m–t** Quantifications of mRNA expressions of *Nfe2l2* (**m, q**), *Keap1* (**n, r**), *Hmox1* (**o, s**), and *Nqo1* (**p, t**) in the mouse HIP at P42 (**m–p**) and P56 (**q–t**). The expressions of responsive genes against oxidative stress were increased in the HIP of METH mice at P42 and P56 after adolescent METH exposure. Data are represented as means (±SEM). Asterisks indicate ***P < 0.001, **P < 0.01, *P < 0.05, unpaired *t*-test and Mann-Whitney test, n = 3–5/condition for inflammatory qPCR, n = 9–13/condition for d-ROMs and BAP tests, n = 9–13/condition for oxidative stress qPCR.

Additionally, adolescent METH exposure increased the number of microglia in the mPFC and dHIP and neuroinflammation. Against neuroinflammation, NFE2L2-mediated redox system was activated in adulthood. Subsequently, we also found increased neurogenesis in the HIP of adult METH mice. Our results demonstrate the long-term impacts of adolescent METH exposure on adult behavior, brain function, neuroinflammation, and body's redox state (Supplementary Fig. 9).

METH is a highly addictive psychostimulant and commonly abused drug [9]. It induces strong stimulating and euphoric effects by increasing DA release and blocking DAT, which reuptakes DA [10, 11]. METH abusers have been reported to show reduced DAT, a marker for DAergic neuron terminals, which correlates with impaired memory and motor function [32]. The DAergic signaling pathway from the VTA regulates processes like reward, pleasure, impulsivity, aggression, motor function, and cognition. The mesolimbic pathway, with DAergic neurons projecting from the VTA to the STR, amygdala (AMY), and HIP, controls emotions, reward, and motivation. A decrease in DA levels in the HIP is linked to anxiety-like behaviors and cognitive impairments [33–35]. As

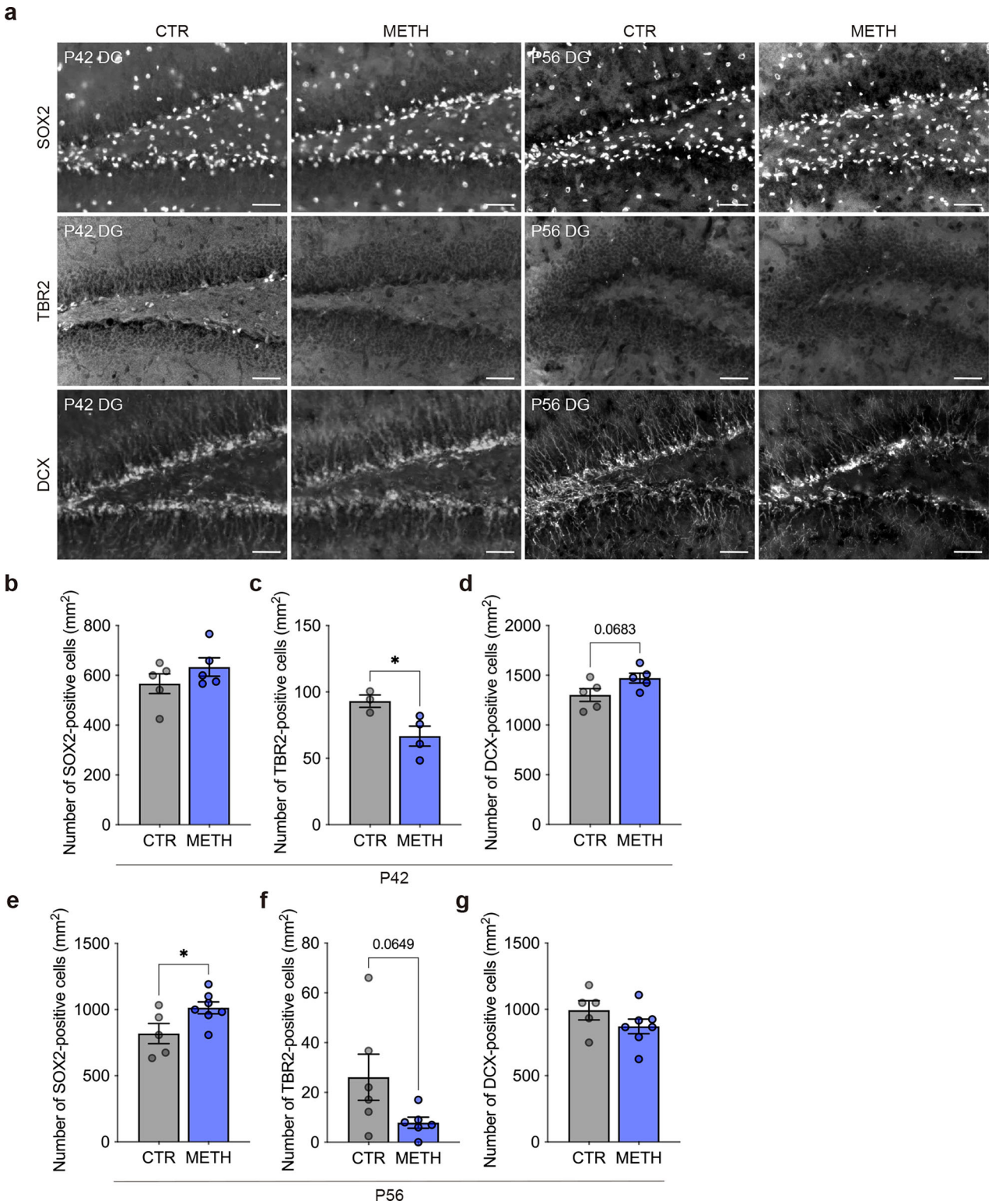

Fig. 5 Enhancement of adult neurogenesis in the DG of adult METH mice. a Representative fluorescence images of adult neural progenitors in the mouse DG at P42 and P56. **b**–**g** Quantifications of SOX2+ (**b, e**), TBR2+ (**c**, **f**), and DCX+ cells (**d**, **g**) at P42 and P56. TBR2+ neural progenitors were reduced in the DG of adult METH mice at P42. On the other hand, SOX2+ neural progenitors were increased in the DG of adult METH mice at P56. Data are represented as means (±SEM). Asterisks indicate **P < 0.01, *P < 0.05, unpaired *t*-test, n = 5/condition. Scale bars: 50 μm.

the functional differences of HIP regions, the dHIP is involved in learning and memory, while the ventral HIP (vHIP) cooperates with the AMY to regulate anxiety-like behaviors [36–38]. The mesocortical pathway, with DAergic neurons projecting from the VTA to the PFC, regulates decision-making, attention, and executive function.

DA systems play a crucial role in controlling adult behaviors, but their plasticity is evident during adolescence, making

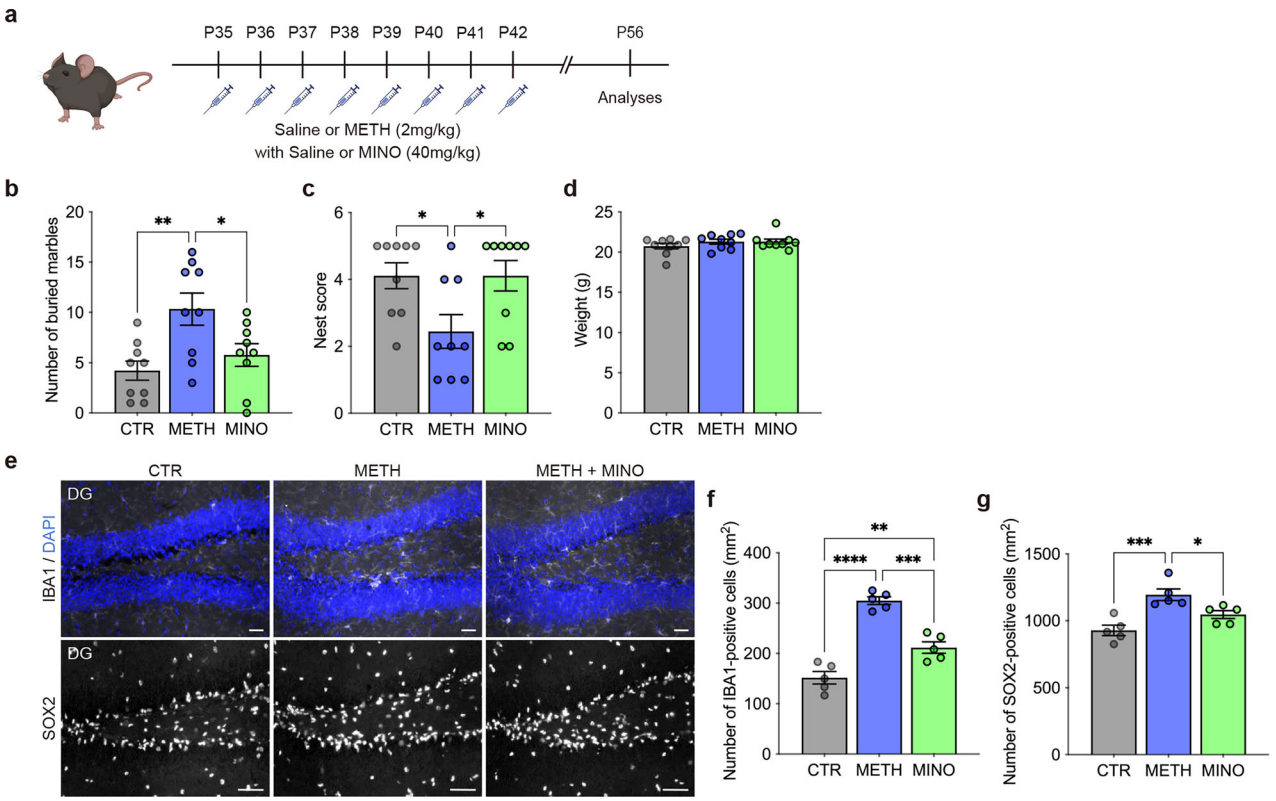

Fig. 6 Microglia inactivation ameliorated adolescent METH-induced phenotypes. a Experimental time course of METH administrations during adolescence. **b** Quantification of the number of buried marbles in the marble-burying test. **c** Quantification of nest score. **d** Quantification of body weight in mice. Adolescent minocycline (MINO) treatment ameliorated METH-induced behavioral abnormalities. **e** Representative fluorescence images of the mouse DG at P56. **f, g** Quantifications of IBA1+ microglia (**f**) and SOX2+ neural progenitors (**g**) in the DG. Adolescent MINO treatment ameliorated METH-induced increases in the number of IBA1+ microglia and SOX2+ neural progenitors. Data are represented as means (±SEM). Asterisks indicate ****P < 0.0001, ***P < 0.001, **P < 0.01, *P < 0.05, one-way ANOVA with a Tukey's multiple comparison test, n = 9/condition for behavioral tests and body weight, n = 5/condition for histological analyses. Scale bars: 50 μm.

abnormalities in DA signaling known to have long-term behavioral effects. Previous study demonstrates that blockade of DAT or monoamine oxidase A (MAOA) from P22–P41 enhances aggression and sensitivity to amphetamine-induced behavioral stimulation in mouse adulthood [39]. Blockade of MAOA during same period also induces anxiety-like behaviors [39]. Recent study has also reported that DAT blockade from P32–P41 increases aggression, impulsivity, and amphetamine sensitivity in adulthood [40]. An increased DAergic activity in VTA is associated with aggression and impulsivity in adult mice [39, 40]. These findings suggest that the DA system is also disrupted in our adolescent METH exposure model (P35-P42), eventually leading to behavioral impairments in adulthood.

METH exposure reduces DA levels in brain regions like the PFC, STR, and HIP [11], leading to behavioral abnormalities associated with these areas. Anxiety-like and cognitive symptoms are common in METH users and animals, especially during the acute withdrawal period, and this is a significant factor contributing to the high relapse rate [41]. Neuroimaging studies of chronic METH users have shown profound structural and functional changes in the brain regions such as PFC, STR, AMY, and HIP associated with sociality, emotion, and cognition, which may explain many of the emotional and cognitive problems seen in these individuals [42–44].

In this study, we demonstrated that adolescent METH exposure results anxiety-like behavior and cognitive impairments in mouse adulthood (Figs. 1, 2). Mice exposed to METH also showed impaired spatial and long-term memory, altered synaptic structure, and fewer CA1 and CA3 neurons during adulthood [45]. Adult METH exposure also increases anxiety-like behaviors and impairs the learning and memory capabilities in adult mice [26, 27, 46]. Previous studies also reported the effects of METH exposure in adolescence. Mice exposed to METH (5 mg/kg) at P11–P20, during HIP development, showed impaired short-term memory but not anxiety-like behaviors at P30 [47]. Mice exposed to METH (4 mg/kg) at P41 exhibited increased anxiety-like behavior and locomotor activity during adolescence without changes in plasma corticosterone levels [48]. Mice exposed to METH (7.5 mg/kg × 4 times) at P30–P31 showed depression-like behaviors and fewer vasopressin + cells in the hypothalamic paraventricular nucleus (PVN) at P41 [49]. Mice exposed to METH (1 and 2 mg/kg) at P35–P48 exhibited impaired spatial and long-term memory in adulthood (P63–P84) [45]. Reduced *Bdnf* mRNA expression was observed in the dHIP of METH mice during adolescence, leading to a decreased number of CA1 and CA3 neurons in adulthood [45]. Additionally, rats exposed to METH (2 mg/kg) at P36–P41 showed anxiety-like behaviors and altered neurogenesis in the dDG in adulthood after 15 days of withdrawal (P56) [50]. Together with our findings, these findings demonstrate that the adult behavioral phenotype we identified is induced by METH, suggesting that the effects of adolescent METH exposure may manifest with a delayed-onset in adulthood.

METH also causes neurotoxicity through mechanisms like oxidative stress, mitochondrial dysfunction, excitability, ER stress, and neuroinflammation, leading to cell death [9, 51, 52]. High doses of METH cause neuronal cell death in the PFC, STR, and HIP, projection sites of DAergic neurons in human and rodents [9, 11, 53, 54]. METH exposure also activates microglia [55–57]. Microglia regulate brain development, repair damage, and control immunity [58, 59]. Microglia also release inflammatory cytokines and mediate neuroinflammation [59]. Reactive microglia

contribute to neurotoxicity by releasing TNFα, IL-1β, and ROS [55]. Previous studies using adult mice show METH increases microglia and proinflammatory cytokines during acute withdrawal [41, 55]. Neuroimaging found METH abuser had over twice the levels of reactive microglia compared to non-users, linking increased microglia to METH neurotoxicity [56].

In this study, we observed an increased phenotype of reactive microglia in the PFC and dHIP in adulthood, but not immediately after low-dose exposure during adolescence (Fig. 3 and Supplementary Fig. 5). These results suggest that microglia activated by adolescent METH exposure contributes to both anxiety-like behaviors and cognitive impairments in adulthood (Figs. 1, 2). It is possible that the increase in microglia in the dHIP and mPFC, where DAergic axon terminals are located, may reflect the consequences of excessive DA signaling and cell damage due to METH-induced oxidative stress. Indeed, the connections between the ventral tegmental area (VTA), PFC, and HIP, centered on the DAergic pathway play the critical roles in regulating the behaviors associated with brain function and psychiatric disorders [60, 61].

Therefore, we inhibited the activation of microglial cells by MINO treatment, which ameliorated the METH-induced phenotype during adolescence (Fig. 6). MINO is a second-generation tetracycline with potent anti-inflammatory and neuroprotective properties that can cross the blood-brain barrier [62]. Previous studies also reported that MINO improved METH-induced hyperlocomotion, cognitive impairments, and neurotoxicity in adult mice through inhibition of microglial activation [63, 64].

High doses of METH cause excessive DA release, disrupting DA metabolism. Extracellular DA is oxidized, producing hydroxyl radical (•OH), hydrogen peroxide (H_2O_2), and reactive oxygen species (ROS), leading to neurotoxicity in axon terminals and surrounding cells due to oxidative stress [55]. In this study, we found increased expressions of oxidative stress response genes in the HIP and decreased reactive oxygen metabolites and increased antioxidant capacity in serum of METH mice in adulthood (Fig. 4). In our experimental system, we did not observe significant neuronal cell death in adult METH mice (Supplementary Fig. 8), likely due to the lower METH dose (2 mg/kg) used in our study compared to other studies (eg. 30, 40 mg/kg) [53, 65].

HMOX1 and NQO1 are critical regulators of redox homeostasis mediated by NFE2L2 [66–71], with KEAP1 serving as a sensor for oxidative stress through its reactive cysteine residues [72]. As downstream effectors of NFE2L2, HMOX1 and NQO1 attenuate oxidative stress and inhibit the production of proinflammatory cytokines, including TNFα, IL-6, and IL-1β [71, 73, 74]. An interesting report on NFE2L2 has demonstrated that oxidative stress induces SOX2 expression in skin keratinocytes, promoting cell proliferation and preventing apoptosis by activating NFE2L2 following cutaneous ischemia [75]. This suggests that SOX2+ neural stem cells may protect themselves from oxidative stress to survive and maintain brain function. Notably, our results show no difference in the number of SOX2+ cells even after adolescent METH exposure (Fig. 5), suggesting that oxidative stress may have induced an increase in SOX2 expression-mediated NFE2L2 expression. It is speculated that adolescent METH exposure stimulates oxidative stress responses, leading to reduced reactive oxygen metabolites and enhanced antioxidant capacity in adult METH mice, promoting neurogenesis in adulthood.

Adolescent METH exposure altered adult neurogenesis in the dDG of METH mice (Fig. 5). We found that decreased TBR2+ intermediate progenitor (Type 2a and 2b) cells and a trend toward an increase in DCX+ intermediate progenitor (Type 2b) and type 3 cells in METH mice at P42. This trend toward a decrease in TBR2+ progenitors were also observed in METH mice at P56, but not in DCX+ progenitors. It has reported that microglia regulates the number of neuronal precursor cells during development by phagocytosis [76], suggesting that the increased number of microglia may have led to a decrease in neural progenitor cells.

In contrast, increased SOX2+ radial glia-like stem (Type 1) cells were only observed in METH mice at P56. Previous study also reported that rats exposed to METH (2 mg/kg) from P36–P41 showed increased DCX+ progenitors in the dDG [50]. Furthermore, it has been reported that neurospheres derived from rat embryo rapidly decrease in the size after exposure to METH, inhibit the G1/S transition and neuronal differentiation, and induce G0/G1 cell cycle arrest [77]. These studies support our hypothesis that adult neural progenitors, after METH exposure, temporarily halt proliferation and later undergo differentiation to replenish neurons in damaged brain regions.

Many previous studies have reported that METH exposure induced neurotoxicity and neuronal cell death in the HIP and other areas [53, 65, 78–80]. On the other hand, other studies have reported that neurogenesis increases during withdrawal from METH exposure [80, 81]. Withdrawal from METH has been reported to increase adult neurogenesis in the DG and play a direct role in context-dependent METH-seeking behavior [80, 82]. Such adult neurogenesis of GCN in the DG is strongly influenced by METH intake and plays a role in seeking behavior [80, 82, 83].

Taken together, our results demonstrate that adult neurogenesis is impaired at P42 immediately after METH exposure but increases at P56 due to a subsequent oxidative stress response, including the induction of SOX2 expression by NFE2L2. Our study provides novel insights into the molecular mechanisms underlies neurogenesis in the DG is increased after METH exposure.

In conclusion, our study demonstrates that adolescent METH exposure has lasting effects on anxiety-like behavior and cognitive decline, accompanied by increased microglial activation and neuroinflammation. Additionally, the persistent elevation of oxidative stress response gene expression triggered with adolescent METH exposure enhances antioxidant capacity, a protective defense system against the damage such as neuroinflammation and oxidative stress, and promotes adult neurogenesis. Our findings offer new insights into the risks of substance use on brain function during adolescence.

DATA AVAILABILITY

The datasets generated during the current study are available from the corresponding author on reasonable request.

REFERENCES

1. Smiley CE, Saleh HK, Nimchuk KE, Garcia-Keller C, Gass JT. Adolescent exposure to delta-9-tetrahydrocannabinol and ethanol heightens sensitivity to fear stimuli. Behav Brain Res. 2021;415:113517.
2. Nakama N, Usui N, Doi M, Shimada S. Early life stress impairs brain and mental development during childhood increasing the risk of developing psychiatric disorders. Prog Neuro-Psychopharmacol Biol Psychiatry. 2023;126:110783.
3. Salmanzadeh H, Ahmadi-Soleimani SM, Pachenari N, Azadi M, Halliwell RF, Rubino T, et al. Adolescent drug exposure: a review of evidence for the development of persistent changes in brain function. Brain Res Bull. 2020;156:105–17.
4. Levine A, Clemenza K, Rynn M, Lieberman J. Evidence for the risks and consequences of adolescent cannabis exposure. J Am Acad Child Adolesc Psychiatry. 2017;56:214–25.
5. D'Amico EJ, Davis JP, Tucker JS, Seelam R, Stein BD. Opioid misuse during late adolescence and its effects on risk behaviors, social functioning, health, and emerging adult roles. Addict Behav. 2021;113:106696.
6. Luna B, Marek S, Larsen B, Tervo-Clemmens B, Chahal R. An integrative model of the maturation of cognitive control. Annu Rev Neurosci. 2015;38:151–70.
7. Luikinga SJ, Kim JH, Perry CJ. Developmental perspectives on methamphetamine abuse: exploring adolescent vulnerabilities on brain and behavior. Prog Neuro-Psychopharmacol Biol Psychiatry. 2018;87:78–84.
8. Volkow ND, Blanco C. Substance use disorders: a comprehensive update of classification, epidemiology, neurobiology, clinical aspects, treatment and prevention. World Psychiatry. 2023;22:203–29.
9. Guo D, Huang X, Xiong T, Wang X, Zhang J, Wang Y, et al. Molecular mechanisms of programmed cell death in methamphetamine-induced neuronal damage. Front Pharmacol. 2022;13:980340.

10. Shrestha P, Katila N, Lee S, Seo JH, Jeong JH, Yook S. Methamphetamine induced neurotoxic diseases, molecular mechanism, and current treatment strategies. Biomed Pharmacother. 2022;154:113591.
11. Sabrini S, Russell B, Wang G, Lin J, Kirk I, Curley L. Methamphetamine induces neuronal death: evidence from rodent studies. Neurotoxicology. 2020;77:20–28.
12. Rusyniak DE. Neurologic manifestations of chronic methamphetamine abuse. Psychiatr Clin North Am. 2013;36:261–75.
13. Tata DA, Yamamoto BK. Interactions between methamphetamine and environmental stress: role of oxidative stress, glutamate and mitochondrial dysfunction. Addiction. 2007;102:49–60.
14. Davidson C, Gow AJ, Lee TH, Ellinwood EH. Methamphetamine neurotoxicity: necrotic and apoptotic mechanisms and relevance to human abuse and treatment. Brain Res Brain Res Rev. 2001;36:1–22.
15. Ghadery C, Pirpamer L, Hofer E, Langkammer C, Petrovic K, Loitfelder M, et al. R2* mapping for brain iron: associations with cognition in normal aging. Neurobiol Aging. 2015;36:925–32.
16. Zweben JE, Cohen JB, Christian D, Galloway GP, Salinardi M, Parent D, et al. Psychiatric symptoms in methamphetamine users. Am J Addict. 2004;13:181–90.
17. Schep LJ, Slaughter RJ, Beasley DM. The clinical toxicology of metamfetamine. Clin Toxicol. 2010;48:675–94.
18. Zhao J, Kral AH, Simpson KA, Ceasar RC, Wenger LD, Kirkpatrick M, et al. Factors associated with methamphetamine withdrawal symptoms among people who inject drugs. Drug Alcohol Depend. 2021;223:108702.
19. Niculescu M, Ehrlich ME, Unterwald EM. Age-specific behavioral responses to psychostimulants in mice. Pharmacol Biochem Behav. 2005;82:280–8.
20. Doi M, Nakama N, Sumi T, Usui N, Shimada S. Prenatal methamphetamine exposure causes dysfunction in glucose metabolism and low birthweight. Front Endocrinol. 2022;13:1023984.
21. Togawa S, Usui N, Doi M, Kobayashi Y, Koyama Y, Nakamura Y, et al. Neuroprotective effects of Si-based hydrogen-producing agent on 6-hydroxydopamine-induced neurotoxicity in juvenile mouse model. Behav Brain Res. 2024;468:115040.
22. Usui N, Berto S, Konishi A, Kondo M, Konopka G, Matsuzaki H, et al. Zbtb16 regulates social cognitive behaviors and neocortical development. Transl Psychiatry. 2021;11:242.
23. Araujo DJ, Toriumi K, Escamilla CO, Kulkarni A, Anderson AG, Harper M, et al. Foxp1 in forebrain pyramidal neurons controls gene expression required for spatial learning and synaptic plasticity. J Neurosci. 2017;37:10917–31.
24. Usui N, Ono Y, Aramaki R, Berto S, Konopka G, Matsuzaki H, et al. Early life stress alters gene expression and cytoarchitecture in the prefrontal cortex leading to social impairment and increased anxiety. Front Genet. 2021;12:754198.
25. Usui N, Matsumoto-Miyai K, Koyama Y, Kobayashi Y, Nakamura Y, Kobayashi H, et al. Social communication of maternal immune activation-affected offspring is improved by si-based hydrogen-producing agent. Front Psychiatry. 2022;13:872302.
26. Struntz KH, Siegel JA. Effects of methamphetamine exposure on anxiety-like behavior in the open field test, corticosterone, and hippocampal tyrosine hydroxylase in adolescent and adult mice. Behav Brain Res. 2018;348:211–8.
27. Ortman HA, Newby ML, Acevedo J, Siegel JA. The acute effects of multiple doses of methamphetamine on locomotor activity and anxiety-like behavior in adolescent and adult mice. Behav Brain Res. 2021;405:113186.
28. Jirkof P. Burrowing and nest building behavior as indicators of well-being in mice. J Neurosci Methods. 2014;234:139–46.
29. McDonnell-Dowling K, Kelly JP. The role of oxidative stress in methamphetamine-induced toxicity and sources of variation in the design of animal studies. Curr Neuropharmacol. 2017;15:300–14.
30. Morrison H, Young K, Qureshi M, Rowe RK, Lifshitz J. Quantitative microglia analyses reveal diverse morphologic responses in the rat cortex after diffuse brain injury. Sci Rep. 2017;7:13211.
31. Ziebell JM, Adelson PD, Lifshitz J. Microglia: dismantling and rebuilding circuits after acute neurological injury. Metab Brain Dis. 2015;30:393–400.
32. Volkow ND, Chang L, Wang GJ, Fowler JS, Franceschi D, Sedler M, et al. Loss of dopamine transporters in methamphetamine abusers recovers with protracted abstinence. J Neurosci. 2001;21:9414–8.
33. Hashikawa-Hobara N, Fujiwara K, Hashikawa N. CGRP causes anxiety via HP1γ-KLF11-MAOB pathway and dopamine in the dorsal hippocampus. Commun Biol. 2024;7:322.
34. Nieoullon A. Dopamine and the regulation of cognition and attention. Prog Neurobiol. 2002;67:53–83.
35. Westbrook A, Braver TS. Dopamine does double duty in motivating cognitive effort. Neuron. 2016;89:695–710.
36. Kjelstrup KG, Tuvnes FA, Steffenach HA, Murison R, Moser EI, Moser MB. Reduced fear expression after lesions of the ventral hippocampus. Proc Natl Acad Sci USA. 2002;99:10825–30.
37. Bannerman DM, Rawlins JN, McHugh SB, Deacon RM, Yee BK, Bast T, et al. Regional dissociations within the hippocampus–memory and anxiety. Neurosci Biobehav Rev. 2004;28:273–83.
38. McHugh SB, Deacon RM, Rawlins JN, Bannerman DM. Amygdala and ventral hippocampus contribute differentially to mechanisms of fear and anxiety. Behav Neurosci. 2004;118:63–78.
39. Yu Q, Teixeira CM, Mahadevia D, Huang Y, Balsam D, Mann JJ, et al. Dopamine and serotonin signaling during two sensitive developmental periods differentially impact adult aggressive and affective behaviors in mice. Mol Psychiatry. 2014;19:688–98.
40. Suri D, Zanni G, Mahadevia D, Chuhma N, Saha R, Spivack S, et al. Dopamine transporter blockade during adolescence increases adult dopamine function, impulsivity, and aggression. Mol Psychiatry. 2023;28:3512–23.
41. Re GF, Li H, Yang JQ, Li Y, Zhang Z, Wu X, et al. Exercise modulates central and peripheral inflammatory responses and ameliorates methamphetamine-induced anxiety-like symptoms in mice. Front Mol Neurosci. 2022;15:955799.
42. Thompson PM, Hayashi KM, Simon SL, Geaga JA, Hong MS, Sui Y, et al. Structural abnormalities in the brains of human subjects who use methamphetamine. J Neurosci. 2004;24:6028–36.
43. Chang L, Alicata D, Ernst T, Volkow N. Structural and metabolic brain changes in the striatum associated with methamphetamine abuse. Addiction. 2007;102:16–32.
44. London ED, Simon SL, Berman SM, Mandelkern MA, Lichtman AM, Bramen J, et al. Mood disturbances and regional cerebral metabolic abnormalities in recently abstinent methamphetamine abusers. Arch Gen Psychiatry. 2004;61:73–84.
45. Liang M, Zhu L, Wang R, Su H, Ma D, Wang H, et al. Methamphetamine exposure in adolescent impairs memory of mice in adulthood accompanied by changes in neuroplasticity in the dorsal Hippocampus. Front Cell Neurosci. 2022;16:892757.
46. Wu L, Liu X, Jiang Q, Li M, Liang M, Wang S, et al. Methamphetamine-induced impairment of memory and fleeting neuroinflammation: profiling mRNA changes in mouse hippocampus following short-term and long-term exposure. Neuropharmacology. 2024;261:110175.
47. Siegel JA, Park BS, Raber J. Long-term effects of neonatal methamphetamine exposure on cognitive function in adolescent mice. Behav Brain Res. 2011;219:159–64.
48. Rud MA, Do TN, Siegel JA. Effects of early adolescent methamphetamine exposure on anxiety-like behavior and corticosterone levels in mice. Neurosci Lett. 2016;633:257–61.
49. Joca L, Zuloaga DG, Raber J, Siegel JA. Long-term effects of early adolescent methamphetamine exposure on depression-like behavior and the hypothalamic vasopressin system in mice. Dev Neurosci. 2014;36:108–18.
50. Loxton D, Canales JJ. Long-term cognitive, emotional and neurogenic alterations induced by alcohol and methamphetamine exposure in adolescent rats. Prog Neuro-Psychopharmacol Biol Psychiatry. 2017;74:1–8.
51. Yang X, Wang Y, Li Q, Zhong Y, Chen L, Du Y, et al. The main molecular mechanisms underlying methamphetamine- induced neurotoxicity and implications for pharmacological treatment. Front Mol Neurosci. 2018;11:186.
52. Kim B, Yun J, Park B. Methamphetamine-induced neuronal damage: neurotoxicity and neuroinflammation. Biomol Ther. 2020;28:381–8.
53. Zhu JP, Xu W, Angulo JA. Methamphetamine-induced cell death: selective vulnerability in neuronal subpopulations of the striatum in mice. Neuroscience. 2006;140:607–22.
54. Golsorkhdan SA, Boroujeni ME, Aliaghaei A, Abdollahifar MA, Ramezanpour A, Nejatbakhsh R, et al. Methamphetamine administration impairs behavior, memory and underlying signaling pathways in the hippocampus. Behav Brain Res. 2020;379:112300.
55. Jayanthi S, Daiwile AP, Cadet JL. Neurotoxicity of methamphetamine: main effects and mechanisms. Exp Neurol. 2021;344:113795.
56. Sekine Y, Ouchi Y, Sugihara G, Takei N, Yoshikawa E, Nakamura K, et al. Methamphetamine causes microglial activation in the brains of human abusers. J Neurosci. 2008;28:5756–61.
57. Thomas DM, Kuhn DM. Attenuated microglial activation mediates tolerance to the neurotoxic effects of methamphetamine. J Neurochemistry. 2005;92:790–7.
58. Li Q, Barres BA. Microglia and macrophages in brain homeostasis and disease. Nat Rev Immunol. 2018;18:225–42.
59. Colonna M, Butovsky O. Microglia function in the central nervous system during health and neurodegeneration. Annu Rev Immunol. 2017;35:441–68.
60. Sigurdsson T, Duvarci S. Hippocampal-prefrontal interactions in cognition, behavior and psychiatric disease. Front Syst Neurosci. 2015;9:190.
61. Kenwood MM, Kalin NH, Barbas H. The prefrontal cortex, pathological anxiety, and anxiety disorders. Neuropsychopharmacology. 2022;47:260–75.
62. Möller T, Bard F, Bhattacharya A, Biber K, Campbell B, Dale E, et al. Critical data-based re-evaluation of minocycline as a putative specific microglia inhibitor. Glia. 2016;64:1788–94.
63. Zhang L, Kitaichi K, Fujimoto Y, Nakayama H, Shimizu E, Iyo M, et al. Protective effects of minocycline on behavioral changes and neurotoxicity in mice after

administration of methamphetamine. Prog Neuro-Psychopharmacol Biol Psychiatry. 2006;30:1381–93.
64. Mizoguchi H, Takuma K, Fukakusa A, Ito Y, Nakatani A, Ibi D, et al. Improvement by minocycline of methamphetamine-induced impairment of recognition memory in mice. Psychopharmacology. 2008;196:233–41.
65. Deng X, Wang Y, Chou J, Cadet JL. Methamphetamine causes widespread apoptosis in the mouse brain: evidence from using an improved TUNEL histochemical method. Brain Res Mol Brain Res. 2001;93:64–69.
66. Motohashi H, Yamamoto M. Nrf2-Keap1 defines a physiologically important stress response mechanism. Trends Mol Med. 2004;10:549–57.
67. Hayes JD, McMahon M. NRF2 and KEAP1 mutations: permanent activation of an adaptive response in cancer. Trends Biochem Sci. 2009;34:176–88.
68. Loboda A, Damulewicz M, Pyza E, Jozkowicz A, Dulak J. Role of Nrf2/HO-1 system in development, oxidative stress response and diseases: an evolutionarily conserved mechanism. Cell Mol Life Sci. 2016;73:3221–47.
69. Kansanen E, Kuosmanen SM, Leinonen H, Levonen A-L. The Keap1-Nrf2 pathway: mechanisms of activation and dysregulation in cancer. Redox Biol. 2013;1:45–49.
70. Ma Q. Role of nrf2 in oxidative stress and toxicity. Annu Rev Pharmacol Toxicol. 2013;53:401–26.
71. Morse D, Lin L, Choi AM, Ryter SW. Heme oxygenase-1, a critical arbitrator of cell death pathways in lung injury and disease. Free Radic Biol Med. 2009;47:1–12.
72. Suzuki T, Muramatsu A, Saito R, Iso T, Shibata T, Kuwata K, et al. Molecular mechanism of cellular oxidative stress sensing by Keap1. Cell Rep. 2019;28:746–58.e744.
73. Rushworth SA, MacEwan DJ, O'Connell MA. Lipopolysaccharide-induced expression of NAD(P)H:quinone oxidoreductase 1 and heme oxygenase-1 protects against excessive inflammatory responses in human monocytes. J Immunol. 2008;181:6730–7.
74. Helou DG, Martin SF, Pallardy M, Chollet-Martin S, Kerdine-Römer S. Nrf2 involvement in chemical-induced skin innate immunity. Front Immunol. 2019;10:1004.
75. Inoue Y, Uchiyama A, Amalia SN, Ishikawa M, Kosaka K, Sekiguchi A, et al. Keratinocyte-Specific SOX2 overexpression suppressed pressure ulcer formation after cutaneous ischemia-reperfusion injury via enhancement of amphiregulin production. J Invest Dermatol. 2024;144:142–51.e145.
76. Cunningham CL, Martínez-Cerdeño V, Noctor SC. Microglia regulate the number of neural precursor cells in the developing cerebral cortex. J Neurosci. 2013;33:4216–33.
77. Wang S, Wang L, Bu Q, Wei Q, Jiang L, Dai Y, et al. Methamphetamine exposure drives cell cycle exit and aberrant differentiation in rat hippocampal-derived neurospheres. Front Pharmacol. 2023;14:1242109.
78. Mandyam CD, Wee S, Crawford EF, Eisch AJ, Richardson HN, Koob GF. Varied access to intravenous methamphetamine self-administration differentially alters adult hippocampal neurogenesis. Biol Psychiatry. 2008;64:958–65.
79. Schmued LC, Bowyer JF. Methamphetamine exposure can produce neuronal degeneration in mouse hippocampal remnants. Brain Res. 1997;759:135–40.
80. Takashima Y, Mandyam CD. The role of hippocampal adult neurogenesis in methamphetamine addiction. Brain Plast. 2018;3:157–68.
81. Recinto P, Samant AR, Chavez G, Kim A, Yuan CJ, Soleiman M, et al. Levels of neural progenitors in the hippocampus predict memory impairment and relapse to drug seeking as a function of excessive methamphetamine self-administration. Neuropsychopharmacology. 2012;37:1275–87.
82. Galinato MH, Takashima Y, Fannon MJ, Quach LW, Morales Silva RJ, Mysore KK, et al. Neurogenesis during abstinence is necessary for context-driven methamphetamine-related memory. J Neurosci. 2018;38:2029–42.
83. Galinato MH, Lockner JW, Fannon-Pavlich MJ, Sobieraj JC, Staples MC, Somkuwar SS, et al. A synthetic small-molecule Isoxazole-9 protects against methamphetamine relapse. Mol Psychiatry. 2018;23:629–38.

ACKNOWLEDGEMENTS

We thank Miyoko Ieki, Stefano Berto, CoMIT Omics Center, and CentMeRE for support.

AUTHOR CONTRIBUTIONS

AI: Validation, Investigation. NU: Conceptualization, Methodology, Validation, Investigation, Writing - Original Draft, Writing - Review & Editing, Visualization, Supervision, Project administration, Funding acquisition. MD: Methodology, Validation, Investigation, Writing - Review & Editing, Funding acquisition. SS: Supervision.

FUNDING

This work was supported by the Japan Society for the Promotion of Science (JSPS) Grant-in-Aid for Scientific Research (B) (23H02837) to N.U.; JSPS Grant-in-Aid for Challenging Research (Exploratory) (24K22230) N.U.; JSPS Grant-in-Aid for Early-Career Scientists (23K14443) to M.D.; Uehara Memorial Foundation to N.U.; Takeda Science Foundation to N.U.; Naito Foundation to N.U.; Mochida Memorial Foundation for Medical and Pharmaceutical Research to N.U.; Inamori Foundation to N.U.; SENSHIN Medical Research Foundation to N.U.; Osaka Medical Research Foundation for Intractable Diseases to N.U. and M.D.; Hirose Foundation to M.D.

COMPETING INTERESTS

The authors declare no competing interests.

ETHICS APPROVAL AND CONSENT TO PARTICIPATE

All experimental procedures were conducted in accordance with the ARRIVE guidelines and relevant institutional regulations. Animal experiments were approved by the Animal Research Committee of The University of Osaka (Approval No. 27-010). This study did not involve human participants; therefore, informed consent was not applicable.

ADDITIONAL INFORMATION

Supplementary information The online version contains supplementary material available at https://doi.org/10.1038/s41398-025-03613-y.

Correspondence and requests for materials should be addressed to Noriyoshi Usui.

Reprints and permission information is available at http://www.nature.com/reprints

Publisher's note Springer Nature remains neutral with regard to jurisdictional claims in published maps and institutional affiliations.